Aerospace Science and Technology 107 (2020) 106269

Contents lists available at ScienceDirect

Aerospace Science and Technology

www.elsevier.com/locate/aescte

Regression rate of paraffin-based fuels in hybrid rocket motor

Lin-lin Liu *, Xiang He, Yin Wang, Ze-bin Chen, Quan Guo

Science and Technology on Combustion, Internal Flow and Thermo-Structure Laboratory, Northwestern Polytechnical University, Xi'an 710072, PR China

ARTICLE INFO

Article history:
Received 23 July 2020
Received in revised form 28 September 2020
Accepted 5 October 2020
Available online 16 October 2020
Communicated by Frank K. Lu

Keywords:
Paraffin-based fuel
Regression rate
Combustion boundary layer
Injector
Hybrid rocket motor

ABSTRACT

Paraffin-based fuels are regarded as a promising solid fuel for hybrid rocket motor (HRM) owing to high regression rate, excellent mechanical performance, and high dropping point. The regression rate of paraffin-based fuels was characterized by static fire test with nitrous oxide (N_2O) and gaseous oxygen (GOX) as oxidizer, and the effect of combustion catalyst, injector and chamber pressure on the regression rate was evaluated in this study. The results show that the average regression rates of paraffin-based fuel with GOX and N_2O are similar under the optimal oxidizer/fuel (O/F) ratio, and the exponent n is larger with GOX as the oxidizer, indicating high sensibility to oxidizer mass flux. The average regression rate increased with the increase in swirling number S_g, and the tangential injector with S_g of 6.83 improved the regression rate significantly. The local regression rate unchanged with axial position when a jet injector was used, but a complex local regression rate appeared at the first half of fuel grain for tangential injector. Both copper chromite and cobalt stearate obviously increased the regression rate; however, only copper chromite could be used as a preferable regression rate improver owing to significant curing acceleration of fuels by cobalt stearate. The average regression rate slightly increased with the increase in chamber pressure with GOX as the oxidizer, but a noticeable positive relationship could be found for the cases of N_2O.

1. Introduction

Hybrid rocket motor (HRM) generally refers to an important chemical aerospace propulsion device with solid fuel and liquid oxidizer as propellant; HRM is characterized by intrinsic safety, high reliability, excellent energy management capability, and low cost [1]. However, HRM with classic polymer fuels such as hydroxyl-terminated polybutadiene (HTPB) [2], polymethyl methacrylate (PMMA) [3], and polythene (PE) [4] usually suffers from a low regression rate, a major obstacle for the application of HRM for a long period [5].

A liquid layer with a low viscosity and surface tension is produced on the burning surface when paraffin is used as the fuel due to a low melting point, and thus droplet entrainment phenomenon occurs, caused by the instability of liquid layer under a high-speed flow. This additional mass transfer mechanism of paraffin does not depend on the heat transfer from high-temperature combustion flame to burning surface, and the regression rate caused by droplet entrainment is usually much higher than that caused by evaporation, resulting in a regression rate 3-4 times higher than classic polymer fuels such as HTPB [6–8]. Therefore, the appearance of paraffin fuel successfully solves the fundamental problem of HRM; this is widely investigated in the field of chemical aerospace propulsion in recent years.

A solid fuel grain is usually affected by vibration and impact loads during the manufacture, storage, transportation, and operation, requiring excellent mechanical performance of fuel grain. In addition, restart performance is achieved based on the high melting point of solid fuel because the structural damage of fuel grain caused by residual heat in the combustion chamber might occur under a low melting point. However, the elongation of paraffin is much lower than that of polymer, and the tensile strength decreases significantly with the increase in temperature. Consequently, solid fuel grain made from pure paraffin can be hardly used in practical HRM.

Classic polymer fuels are characterized by excellent mechanical performance, especially under a high temperature, and one of the most effective methods to improve the performance of paraffin is the addition of a polymer into paraffin. Yuki et al. used PMMA powder as the additive of paraffin. Addition of PMMA increased the tensile strength of fuel; however, the regression rate decreased as the addition amount was increased due to a higher viscosity of melting layer [9]. Kim et al. invented a novel blended solid fuel by mixing paraffin with polyethylene. Experimental results showed that the fuel can be regarded comparatively effective for HRM in

* Corresponding author.
E-mail address: lll@nwpu.edu.cn (L.-l. Liu).

https://doi.org/10.1016/j.ast.2020.106269

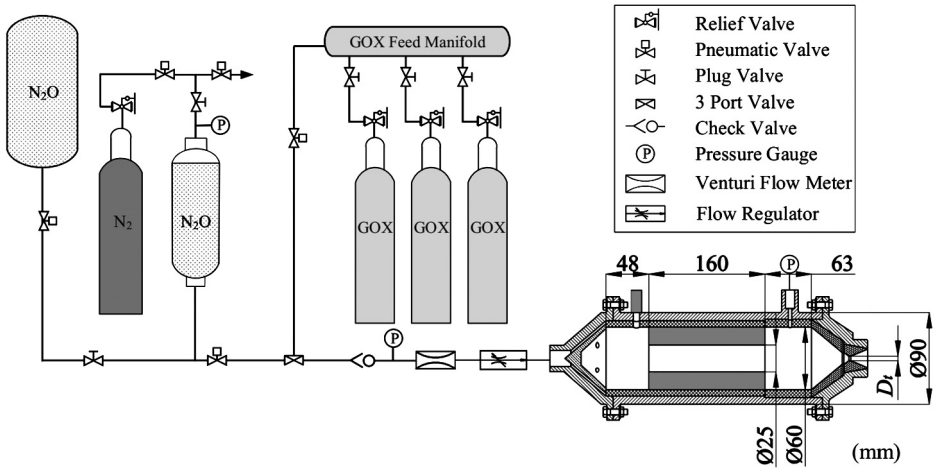

Fig. 1. Schematic of static fire system.

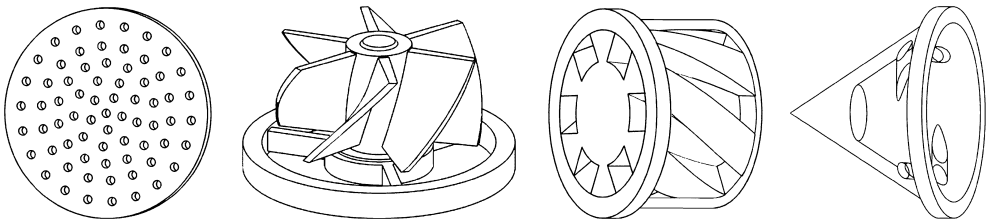

Fig. 2. Injectors used in this study.

terms of mechanical strength, combustion efficiency, and combustion instability [10,11].

Mengu et al. used the copolymer of ethylene vinyl acetate (EVA) and styrene-ethylene-butylene-styrene (SEBS) to enhance the performance of paraffin. Paraffin mixed with a combination of 10% SEBS and 5% EVA showed the best regression rate characteristics and mechanical properties. In addition, combustion efficiency increased in the presence of polymeric additives [12]. Six types of additives including stearic acid, polyethylene wax, EVA, low density polyethylene (LDPE), high density polyethylene (HDPE), and polypropylene (PP) were blended in paraffin fuel. The mechanical properties of fuels improved; however, all the additives except stearic acid reduced the regression rate of fuels due to increased melted liquid viscosity [13]. Wu et al. invented a new paraffin-based solid fuel with favorable mechanical strength, consisting of 50 wt% paraffin, 20 wt% PE wax, 18 wt% EVA, 10 wt% SA and 2 wt% carbon [14].

HTPB is the most common used binder of composite solid propellant, and it is also widely used as a solid fuel for HRM. Although the regression rate of HTPB is much lower than that of paraffin, it can be used as an additive to enhance the mechanical performance and melting point of paraffin. Lee et al. developed various solid fuels with different weight ratios of paraffin wax and HTPB mixtures. 70P fuel (70% paraffin + 30% HTPB) maintained stable combustion under most test conditions. 50P fuel showed about 61% increase in regression rate compared to HTPB under swirling GOX injection [15]; however, a similar low regression rate is observed under a high content of HTPB [16]. Solid fuels can also be prepared by suspending paraffin particles in HTPB, exhibiting adequate thermal and mechanical properties for a HRM [17].

Regression rate is a key parameter for both solid fuel and HRM [18]. Formulation and microstructure of paraffin-based fuel are different from those of paraffin or polymer, resulting in different regression rate characteristics. Combustion of solid fuel in HRM is characterized by diffusion combustion located in turbulent boundary layer. Thus, the local regression rates at different axial distances are usually much different from each other due to a significant difference in the nature of boundary layer [19–21]. Paraffin-based fuels with different formulas were prepared with paraffin, HTPB, and metal powder as the main raw materials, and the local and average regression rates of fuels were investigated in this study. This study might help to elucidate the combustion mechanism and to develop solid fuel and HRM.

2. Experiment

2.1. Paraffin-based fuel formulas

The ingredients of baseline formulation (namely, 1# solid fuel) in this study are solid paraffin 38 wt%, liquid paraffin 28 wt%, improved PE 4 wt%, HTPB matrix 15 wt%, aluminum with a particle size of 10 μm 10 wt%, and magnesium with a particle size of 1 μm 5 wt%. Semi-refined solid paraffin and liquid paraffin were purchased from Daqing Petrochemical Company and Sinopharm Chemical Reagent Co., Ltd., respectively. HTPB was cured by toluene-2,4-diisocyanate (TDI) and triphenyl bismuth (TPB) as the curing catalyst. To improve the combustion performance of solid fuel, catocene, copper chromite, and cobalt stearate of 1 wt% were used as the combustion catalyst, namely, 2#, 3#, and 4# solid fuel, respectively. The content of solid paraffin decreased by 1 wt% to ensure the total content of 100 wt% in these three formulations. The fuel formulation are shown in Table 1.

Solid paraffin, liquid paraffin, HTPB and improved PE were first mixed in mixer at 120 °C for 3 h to form the liquid slurry, then aluminum, magnesium and TDI were added when the temperature dropped to 80 °C. Vacuum casting of fuel slurry was carried out after stirring for 1 h, and the fuel grains were successfully manufactured finally after the curing of 5 days at 70 °C.

Table 1
Paraffin-based fuels formulation.

No.	Matrix (%)	Paraffin (%)	Improved PE (%)	Mg (%)	Al (%)	Catalyst
1#	15	66	4	5	10	–
2#	15	65	4	5	10	catocene
3#	15	65	4	5	10	copper chromite
4#	15	65	4	5	10	cobalt stearate

2.2. Experimental facility

Gaseous oxygen (GOX) and nitrous oxide were used as the oxidizers in this study. The feeding system is shown in Fig. 1.

Three or more bottles of GOX with a high pressure were connected in parallel to satisfy the requirement of mass flux of oxidizer. Orifices of different effective flow areas were used to evaluate and regulate the mass flow rate of GOX.

N_2O is a storable liquid oxidizer commonly used in HRM, and the system can also supply the motor with N_2O of stable mass flow rate. High pressure (more than 7 MPa) nitrogen was used to extrude N_2O, and the measurement and regulation of mass flow rate were achieved using a venturi tube.

The motor mainly consists of an injector, a pre-combustion chamber, a main combustion chamber, a post-combustion chamber, and a nozzle. Graphite was used as the thermal insulation blanket of combustion chamber and the nozzle material. In addition, single port tubular solid fuel grain was loaded in the main combustion chamber. The injected oxidizer mixed and combusted with gasified fuels in the combustion chamber, and the regression rate of solid fuel was mainly affected by the heat feedback from high-temperature combustion flame to burning surface. Therefore, the gas flow optimization by injector improved the regression rate. The swirl number (S_g) could characterize the swirling intensity of the injector, and can be calculated through the method presented in reference [22]. Four injectors with different S_g used in this study are shown in Fig. 2.

2.3. Evaluation of regression rate from static fire testing

The combustion was quenched by interrupting the supply of oxidizer. Then, the regression rate of solid fuel was obtained by combining the difference in mass or inner diameter of fuel grain before or after the combustion and combustion time. The average regression rate $\bar{r}$ can be expressed as follows:

$$\bar{r} = \frac{\sqrt{D^2 - \frac{4(m_1 - m_2)}{\pi L \rho_f}} - d}{t_c} \tag{1}$$

where D, d, m_1, and L are the outer diameter, inner diameter, mass, and length of unburned fuel grain, respectively; m_2 and ρ_f are the residual mass and density of fuel grain, respectively; t_c is burning time, which can be obtained from the pressure-time curve of static fire experiments, as shown in Fig. 3.

In general, the relationship between regression rate and oxidizer mass flux G_o can be expressed by the following empirical formula:

$$r = aG_o^n \tag{2}$$

where a is the regression rate constant and n is the exponent. The values of a and n could be obtained by fitting the regression rate under different oxidizer mass flux. G_o can be calculated using Equation (3):

$$G_o = \frac{\dot{m}}{A_b} \tag{3}$$

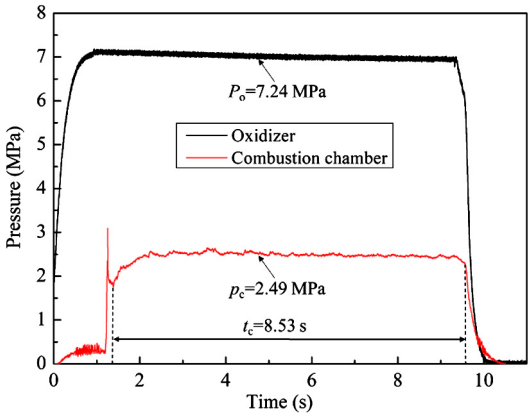

Fig. 3. One static fire testing result with GOX as oxidizer.

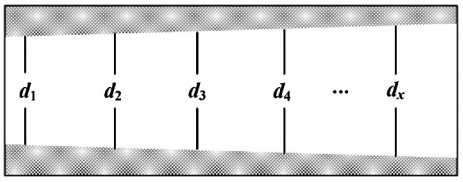

Fig. 4. Quenched fuel grain schematic.

where $\dot{m}$ is the mass flow rate of oxidizer and A_b is the port area of fuel grain.

The relationship between r and G_o could be obtained by the linear fitting of the logarithmic form of equation (2).

$$\ln r = \ln a + n \ln G_o \tag{4}$$

The regression rate mainly depends on the characteristics of combustion boundary layer above the burning surface, and it varies with the axial position of fuel grain, i.e., the local regression behavior.

Fig. 4 shows a schematic diagram of quenched fuel grain, and the local regression r_x can be obtained from the local inner diameter, outer diameter, and burning time.

$$r_x = \frac{d_0 - dx}{2t_c} \tag{5}$$

3. Results and discussions

3.1. Regression rate characteristics of paraffin-based fuels

GOX has a strong oxidation capacity. Severe nozzle ablation occurred due to the low combustion efficiency when the jet injector was used [23]. Therefore, a tangential injector with $S_g = 6.83$ was used to show the regression rate characteristics of 3# paraffin-based fuels with GOX and N_2O as the oxidizer, and the average regression rate $\bar{r}$ results are shown in Table 2.

The fitting results of the data in Table 2 are shown in Fig. 5.

Table 2 shows that the average regression rate $\bar{r}$ has a positive relationship with oxidizer mass flux due to diffusion combustion mechanisms, and the value of $\bar{r}$ increased from 0.45 mm·s^{-1}

Table 2
Average regression rate of 3# paraffin-based fuel.

No.	Oxidizer	G_o (kg·m^{-2}·s^{-1})	$\bar{r}$ (mm·s^{-1})
1	GOX	24.91	0.45
2	GOX	33.53	0.51
3	GOX	39.75	0.59
4	GOX	40.63	0.60
5	GOX	58.54	0.88
6	N_2O	91.00	0.45
7	N_2O	96.22	0.54
8	N_2O	138.56	0.56
9	N_2O	171.72	0.59
10	N_2O	241.74	0.78

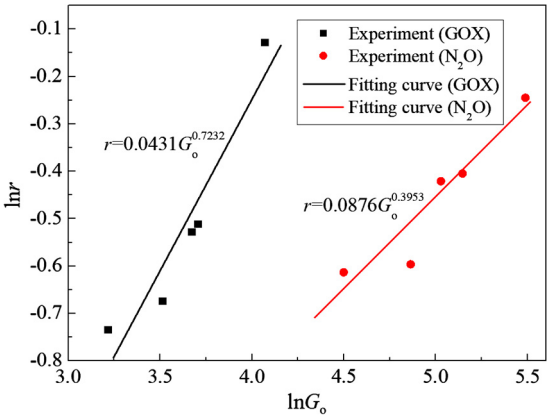

Fig. 5. Curve of regression rate.

to 0.88 mm·s^{-1} with the increase in oxidizer flux from 24.91 kg·m^{-2}·s^{-1} to 58.54 kg·m^{-2}·s^{-1}. The empirical formula of regression rate fitted using Equation (4) can be expressed as follows:

$$r = 0.0431 G_o^{0.7232} \tag{6}$$

The average regression rate $\bar{r}$ increased from 0.45 mm·s^{-1} to 0.78 mm·s^{-1} when the mass flux of N_2O increased from 91.00 kg·m^{-2}·s^{-1} to 241.74 kg·m^{-2}·s^{-1}, and the relationship between regression rate and oxidizer mass flux can be expressed as follows:

$$r = 0.0876 G_o^{0.3953} \tag{7}$$

Equations (6) and (7) show that exponent n is larger with GOX as the oxidizer, i.e., a high sensibility to oxidizer mass flux. This is because of a high oxidation capacity and less heat required during the injection for GOX. Meanwhile, the constant a becomes smaller with GOX as the oxidizer, indicating a lower regression rate; however, the regression rates are similar under the optimal oxidizer/fuel (O/F) ratio for both oxidizers.

The quenched fuel grains with GOX and N_2O as the oxidizer were cut along the axial direction to expose the burned grain pattern. Fig. 6 shows the axial view of split quenched fuel grains.

Fig. 6 shows that the regression rate varied with the axial position, while it remained nearly invariant for different circumferential and same axial positions. Therefore, thin slices were cut off from half fuel grains, and the residual thickness of solid fuel was obtained using point-by-point mapping. The original photograph and mapping picture of slices are shown in Figs. 7 and 8, respectively.

Axial local inner diameter of quenched fuel grain could be easily obtained from the coordinate values, and consequently the local regression rate was evaluated. The uneven burning surface shown in Figs. 7 and 8 indicates an obvious difference in the axial local regression rate, the relationship between local regression rate and axial position is shown in Fig. 9.

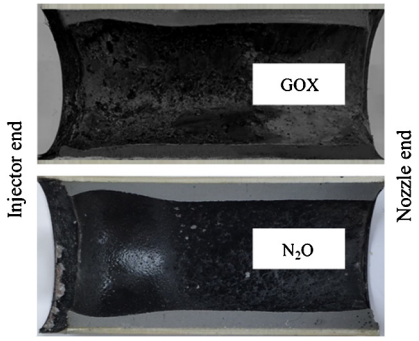

Fig. 6. Axial view of quenched fuel grains.

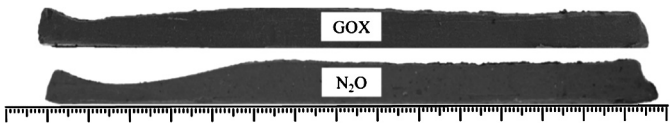

Fig. 7. Photograph of slices.

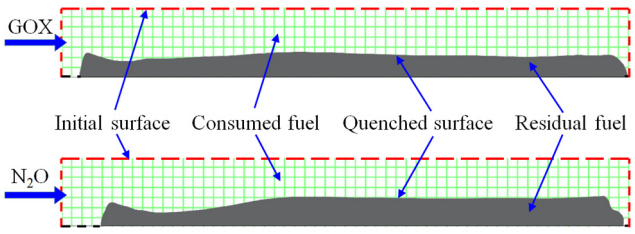

Fig. 8. Mapping picture of slices.

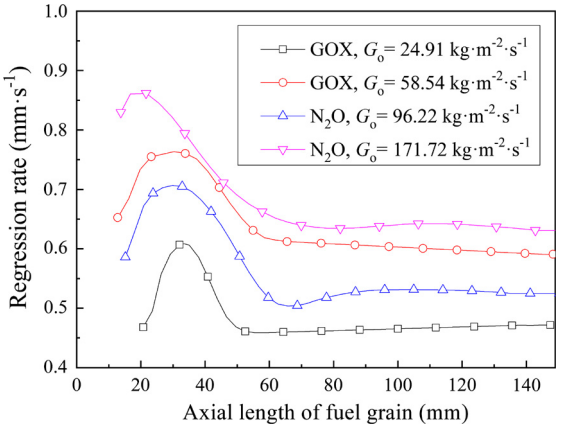

Fig. 9. Local regression rate of paraffin-based fuels.

Fig. 9 shows that the local regression rate first increased and then decreased to the level of average regression rate of the latter part of fuel grain, forming an obvious pit nearby the injector end of fuel grain. The regression rate of paraffin-based fuels was mainly determined by the gasification of HTPB through thermal decomposition, the evaporation of paraffin, and the entrainment of paraffin droplet. The first two mass addition processes depended on the heat feedback from the high-temperature combustion flame, while the latter one was determined by the gas flow velocity. A thin turbulent boundary layer and strong swirling gas flow near the axial position of injector would enhance the heat feedback, although a low flame temperature is caused by the high O/F. This results in a medium local regression rate. More reasonable O/F was achieved with the increase in axial position. Thus, the local regression rate increased due to a higher heat feedback.

Table 3
Average regression rate of different formulas.

Solid fuel	Oxidizer	G_o (kg·m^{-2}·s^{-1})	$\bar{r}$ (mm·s^{-1})
1#	GOX	40.27	0.43
2#	GOX	38.03	0.44
3#	GOX	40.63	0.60
4#	GOX	39.23	0.57
1#	N_2O	87.27	0.42
3#	N_2O	89.98	0.54
4#	N_2O	89.98	0.54

When the axial length was further increased, the gas flow velocity increased. This favors the entrainment of paraffin droplet. However, the swirling of gas was significantly weakened due to the viscosity of gas, mass addition from solid fuel, and friction on burning surface, resulting in the thickening of boundary layer. Therefore, the local regression rate gradually decreased, mainly because of the lower heat feedback might be resulted from the weakened swirling gas.

In the middle and downstream, the swirling of gas flow was further weakened. Thus, the regression rate was mainly affected by the boundary layer thickness and paraffin droplet entrainment. The boundary layer thickness slowly increased with axial distance, and the entrained paraffin droplet also increased by the gradually increased total mass flux due to the accumulation of combustion products [7]. The thick boundary layer negatively affected the regression rate because of the lower heat feedback to burning surface, while the increased entrained paraffin droplet played a positive role. Thus, a slight change in local regression rate appeared with axial position as the combining results of both different effects.

In addition, no residual fuel was observed nearby the injector end and nozzle end of fuel grain, indicating a much higher local regression rate. This is because of a strong backflow of high-temperature combustion gas at these axial positions, and this can also be attributed to a higher local regression rate in the tail of quenched solid fuel.

3.2. Effect of combustion catalyst on the regression rate

The optimal O/F ratios of GOX/paraffin-based fuel and N_2O/paraffin-based fuel are about 1.9 and 5.3, respectively. Thus, the oxidizer mass flux was selected as about 40 kg·m^{-2}·s^{-1} and 90 kg·m^{-2}·s^{-1}, respectively. The average regression rate of different formulas under tangential injector is shown in Table 3.

Table 3 shows that catocene slightly affected the regression rate of solid fuel although it is widely used in composite solid propellants as a burning rate improver. Both copper chromite and cobalt stearate exhibited similar positive effect on the regression rate and clearly enhanced the regression rate. 1 wt% of copper chromite and cobalt stearate increased the regression rate by 39.5% and 32.6% for GOX, respectively, while 28.6% for N_2O. Therefore, both copper chromite and cobalt stearate are preferable regression rate improvers of paraffin-based fuels; however, a small amount of cobalt stearate accelerated the curing of fuels significantly. The viscosity of slurry for 4# fuel increased remarkable within 1 h after the completion of mixing, which is unfavorable for the vacuum casting of fuel slurry.

3.3. Effect of injector on regression rate

The regression of solid fuels in HRM mainly depends on the heat feedback from high-temperature combustion flame to burning surface. The streamline of injected oxidizer is much important for combustion in fuel grain ports and might have obvious effect on the regression rate [24,25]. Four injectors were used in this study to evaluate the streamline of oxidizer on the regression rate of 3# solid fuel, and the average regression rates are shown in Table 4.

Table 4
Average regression rate with different injectors.

No.	Injector	Oxidizer	G_o (kg·m^{-2}·s^{-1})	$\bar{r}$ (mm·s^{-1})
1	jet	GOX	40.27	0.39
2	turbine rotor	GOX	34.87	0.29
3	turbine rotor	GOX	39.19	0.32
4	spiral groove	GOX	41.90	0.48
5	tangential	GOX	40.63	0.60
6	jet	N_2O	87.62	0.44
7	jet	N_2O	154.76	0.53
8	tangential	N_2O	89.98	0.54
9	tangential	N_2O	152.73	0.66

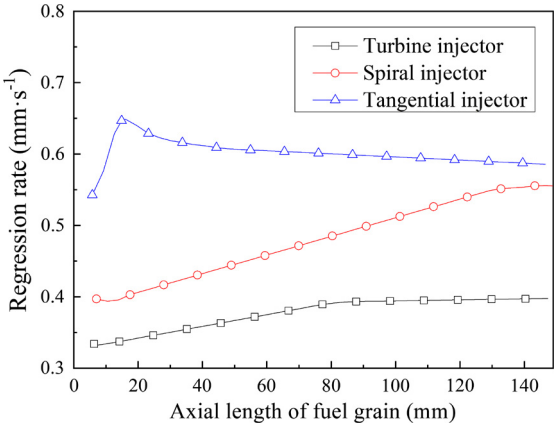

Fig. 10. Local regression rate with GOX as oxidizer.

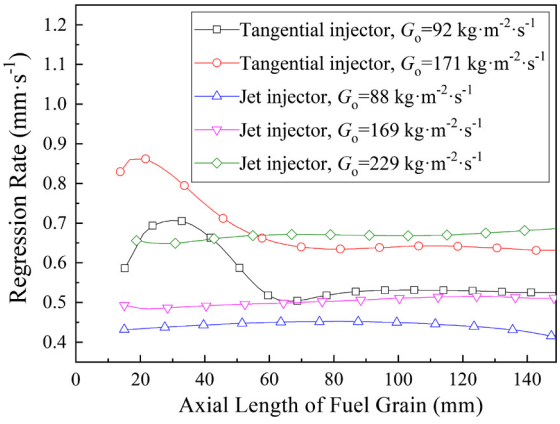

Fig. 11. Local regression rate with N_2O as oxidizer.

The flow path of oxidizer could be lengthened and distance between the oxidizer and burning surface could be shortened under the centrifugal force when swirling injectors are used. This is beneficial for improving both regression rate and combustion efficiency. Table 4 shows that both spiral groove injector ($S_g = 1.92$) and (especially) tangential injector ($S_g = 6.83$) clearly improved the regression rate, and the larger the swirling number S_g, the higher the regression rate. Tangential injector increased the regression rate by 53.8% with GOX as the oxidizer, while 22.7% and 24.5% for N_2O mass flux of about 87.62 kg·m^{-2}·s^{-1} and 152.73 kg·m^{-2}·s^{-1}. The gaseous reaction rate of gasified fuels with GOX is extremely high owing to strong oxidation capacity, and the combustion is mainly controlled by aerodynamics rather than chemical kinetics. Therefore, the swirling injector might be more efficient for GOX by improving diffusion.

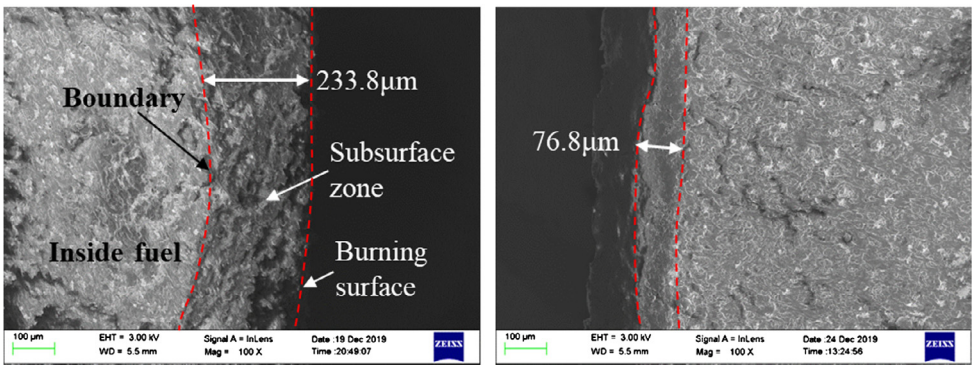

a) with jet injector b) with tangential injector

Fig. 12. SEM images of quenched fuels with different injectors.

Table 4 also shows that the lowest regression rate was achieved when a turbine rotor injector was used, although the swirling flow of oxidizer could also be formatted. This is probably because the gas flow in the fuel grain port was strongly disturbed by the swirling flow of oxidizer, and then a stable turbulent boundary layer could not be formed. This is unfavorable for the heat feedback to burning surface and consequently regression rate.

The effect of streamline on the local regression rate of paraffin-based fuels was also investigated by analyzing the slices obtained from static fire testing shown in Table 4. The results are shown in Figs. 10 and 11.

Fig. 10 shows that the local regression rate linearly increased in general in the case of a spiral groove with the increase in axial position, while it increased first linearly and then remained constant in the case of a turbine rotor. This is significantly different from a tangential injector. A relatively small deviation was observed in the local regression rate from average regression for turbine rotor and tangential injector, and a lower regression rate was achieved when a turbine rotor injector was used. Therefore, a tangential injector could be used as a preferable injector of GOX only after the optimization of fuel grain port configuration.

Fig. 11 shows a negligible change in the local regression rate with the change in axial position when a jet injector was used, indicating a stable heat feedback from combustion flame to burning surface in the absence of swirling, especially at the axial position nearby the injector end of fuel grain. However, as mentioned above, complex changes in local regression rate occurred with the increase in axial distance when a tangential injector was used, particularly to the first half of fuel grain in general. In addition, Fig. 10 and Fig. 11 indicate that the variation in local regression rate was more obvious when N_2O was used as the oxidizer. This is because the disturbance of swirling to boundary layer was weakened by a high reaction capacity and low inertia force of oxygen molecules.

Fuel grain slices were analyzed by scanning electron microscopy (SEM), and the radial profile of quenched 3# paraffin-based fuel (samples were obtained from test No. 7 and test No. 9 of Table 4) is shown in Fig. 12.

Fig. 12 shows an obvious subsurface reaction zone during combustion, and the reactions in this zone were mainly due to the melting of solid paraffin because of the low temperature at burning surface. The thicker the subsurface reaction zone, the higher the burning surface temperature (more heat feedback from combustion flame). Therefore, the thickness of subsurface reaction zone should have a positive relationship with regression rate. This is consistent with the results shown in Fig. 12.

3.4. Effect of chamber pressure on regression rate

The combustion of HRM is characterized by diffusion combustion owing to a feature of propellant that oxidizer and fuel are separately stored and have different phases, and then the regression rate is usually mainly controlled by oxidizer mass flux rather than chamber pressure. However, the gaseous-phase reaction rate in the boundary layer is positively correlated with pressure, and thus the chamber pressures may also have an influence on the regression rate through the changes of heat feedback from the combustion flame to the burning surface. Therefore, the regression rate is usually mainly controlled by oxidizer mass flux rather than chamber pressure. However, the gaseous-phase reaction rate in the boundary layer is significantly influenced by pressure, and the chamber pressure still had some influence on the regression rate. Nozzles of different throat diameters were used to regulate the chamber pressure, and 3# solid fuel and tangential injector were used in this study. Table 5 shows the results of average regression rate.

Table 5
Average regression rate under different pressures.

No.	Oxidizer	G_o (kg·m^{-2}·s^{-1})	p_c (MPa)	$\bar{r}$ (mm·s^{-1})
1	GOX	39.75	1.52	0.57
2	GOX	40.89	2.63	0.59
3	GOX	40.47	2.96	0.64
4	GOX	43.86	3.61	0.69
5	N_2O	219.67	1.25	0.41
6	N_2O	229.34	1.89	0.56
7	N_2O	200.93	3.40	0.61
8	N_2O	201.01	4.20	0.71

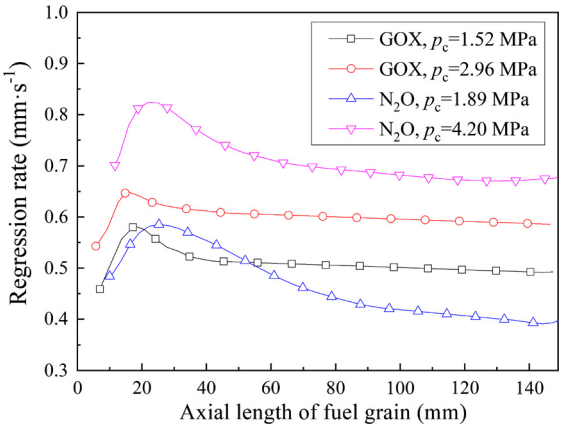

Fig. 13. Local regression rate under different chamber pressures.

Table 5 shows that the average regression rate with GOX as the oxidizer increased from 0.57 mm·s^{-1} to 0.69 mm·s^{-1} when the chamber pressure increased from 1.52 MPa to 3.61 MPa, indicating a weak positive correlation between operation pressure and regression rate. However, Table 5 also shows a noticeable increased average regression rate when N_2O was used as the oxidizer under

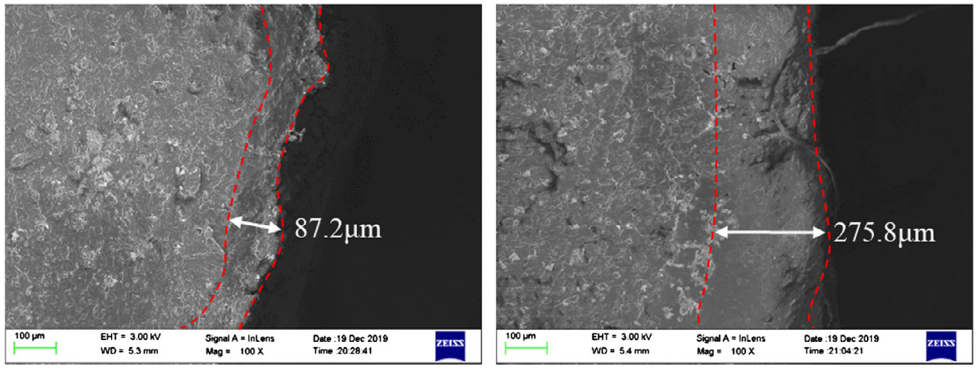

a) p_c=1.91 MPa b) p_c=3.10 MPa

Fig. 14. SEM images of quenched fuels under different operation pressures.

a higher chamber pressure, and the regression rate increased by 73.2% when the chamber pressure increased from 1.25 MPa to 4.20 MPa.

The higher gaseous reaction rate resulted from a higher chamber pressure which would shorten the distance between combustion flame and burning surface. The regression rate increased due to a higher heat feedback to burning surface. Therefore, the higher the chamber pressure, the higher the regression rate. In addition, a much higher reaction rate can be achieved for the reactions between gasified fuels and GOX, and then the heat feedback from the combustion flame to the burning surface was more dependent on the aerodynamics, resulting in the insensitivity to chamber pressure.

Fig. 13 shows the local regression rates from static fire testing shown in Table 5 (No. 1, No. 3, No. 6, No. 8).

Fig. 13 shows that the chamber pressure only affected the value of local regression rate, but it did not affect the variation trend with the axial position.

Fig. 14 shows the SEM images of fuel grain slices, demonstrating the subsurface profile of quenched 3# paraffin-based fuel under different operation pressures.

Fig. 14 shows that the thickness of subsurface zone significantly increased with the increase in chamber pressure, directly caused by the enhanced heat feedback to burning surface. Therefore, the thicker subsurface reaction zone under a higher chamber pressure can confirm the hypothesis that explains the effect of chamber pressure on regression rate.

Conclusions

(1) The average regression rates of paraffin-based fuel with GOX and N_2O are similar under the optimal O/F ratio, and the exponent n is larger with GOX as the oxidizer for the tangential injector owing to a high oxidation capacity and requirement of less heat during the injection, i.e., high sensibility to oxidizer mass flux.

(2) Average regression rate increased with the increase in swirling number S_g, and the tangential injector with S_g of 6.83 significantly improved the regression rate. The local regression rate basically remained unchanged with axial position when a jet injector was used; however, an obvious higher local regression rate was observed at the first half of fuel grain when a tangential injector was used, forming an obvious pit nearby the injector end of fuel grain.

(3) Both copper chromite and cobalt stearate improved the regression rate and enhanced the regression rate obviously, but only copper chromite could be used as a preferable regression rate improver due to a significant curing acceleration of fuels by cobalt stearate even in a small amount.

(4) A weak positive correlation was observed between operation pressure and average regression rate with GOX as the oxidizer, while a noticeable increased average regression rate was observed under a higher chamber pressure for the cases of N_2O. The reactions between gasified fuels and GOX were mainly controlled by aerodynamics rather than chemical kinetics, resulting in the insensitivity of regression rate to chamber pressure.

Declaration of competing interest

The authors declare that they have no known competing financial interests or personal relationships that could have appeared to influence the work reported in this paper.

Acknowledgement

This work is supported by National Natural Science Foundation of China (Grant No. 51976175 and 51606157).

References

[1] D. Altman, Overview and history of hybrid rocket propulsion, in: Fundamentals of Hybrid Rocket Combustion and Propulsion, American Institute of Aeronautics and Astronautics, 2007, pp. 1–36.
[2] J. Arves, H. Jones, K. Kline, K. Smith, T. Slack, T. Bales, J. Arves, H. Jones, K. Kline, K. Smith, T. Slack, T. Bales, Development of a N2O/HTPB hybrid rocket motor, in: 33rd Joint Propulsion Conference and Exhibit, American Institute of Aeronautics and Astronautics, 1997.
[3] S. Yuasa, K. Yamamoto, H. Hachiya, K. Kitagawa, Y. Oowada, Development of a small sounding hybrid rocket with a swirling-oxidizer-type engine, in: Joint Propulsion Conference and Exhibit, 2001, pp. 248–251.
[4] S. Zhao, G. Cai, H. Tian, N. Yu, P. Zeng, Experimental tests of throttleable H_2O_2PE hybrid rocket motors, in: 51st AIAA/SAE/ASEE Joint Propulsion Conference, American Institute of Aeronautics and Astronautics, 2015.
[5] M.J. Chiaverini, N. Serin, D.K. Johnson, Y.-C. Lu, K.K. Kuo, G.A. Risha, Regression rate behavior of hybrid rocket solid fuels, J. Propuls. Power 16 (2000) 125–132.
[6] M.A. Karabeyoglu, D. Altman, B.J. Cantwell, Combustion of liquefying hybrid propellants: Part 1, general theory, J. Propuls. Power 18 (2002) 610–620.
[7] M.A. Karabeyoglu, B.J. Cantwell, Combustion of liquefying hybrid propellants: Part 2, stability of liquid films, J. Propuls. Power 18 (2002) 621–630.
[8] A. Karabeyoglu, G. Zilliac, B.J. Cantwell, S. Dezilwa, P. Castellucci, Scale-up tests of high regression rate paraffin-based hybrid rocket fuels, J. Propuls. Power 20 (2012) 1037–1045.
[9] Y. Matsumoto, K. Takahashi, K. Kinoshita, K. Nakajima, Characteristics of a polymeric as an additive in WAX-based hybrid rocket fuel, in: 2018 Joint Propulsion Conference, 2018.
[10] S. Kim, J. Lee, H. Moon, H. Sung, J. Kim, J. Cho, Effect of paraffin-LDPE blended fuel on the hybrid rocket motor, in: 46th AIAA/ASME/SAE/ASEE Joint Propulsion Conference & Exhibit, 2012.
[11] S. Kim, H. Moon, J. Kim, J. Cho, Evaluation of paraffin–polyethylene blends as novel solid fuel for hybrid rockets, J. Propuls. Power 31 (2015) 1750–1760.
[12] D. Mengu, R. Kumar, Development of EVA-SEBS based wax fuel for hybrid rocket applications, Acta Astronaut. 152 (2018) 325–334.
[13] Y. Tang, S. Chen, W. Zhang, R. Shen, L.T. DeLuca, Y. Ye, Mechanical modifications of paraffin-based fuels and the effects on combustion performance, Propellants Explos. Pyrotech. 42 (2017) 1268–1277.

[14] Y. Wu, X. Yu, X. Lin, S. Li, X. Wei, C. Zhu, L. Wu, Experimental investigation of fuel composition and mix-enhancer effects on the performance of paraffin-based hybrid rocket motors, Aerosp. Sci. Technol. 82 (2018) 620–627.
[15] T.-S. Lee, H.-L. Tsai, Combustion characteristics of a paraffin-based fuel hybrid rocket, in: 9th Asia-Pacific International Symposium on Combustion and Energy Utilization, 2008, pp. 2–6.
[16] R. Sakote, N. Yadav, S. Karmakar, P.C. Joshi, A.K. Chatterjee, Regression rate studies of paraffin Wax-HTPB hybrid fuels using swirl injectors, Propellants Explos. Pyrotech. 39 (2014) 859–865.
[17] K.P. Cardoso, L.F. Ferrão, E.Y. Kawachi, T.B. Araújo, R.F. Nunes, M.Y. Nagamachi, Preparation of paraffin-based solid combustible for hybrid propulsion rocket motor, J. Propuls. Power 33 (2017) 448–455.
[18] H. Tian, Y. Li, C. Li, X. Sun, Regression rate characteristics of hybrid rocket motor with helical grain, Aerosp. Sci. Technol. 68 (2017) 90–103.
[19] G. Marxman, M. Gilbert, Turbulent boundary layer combustion in the hybrid rocket, in: Symposium (International) on Combustion, Elsevier, 1963, pp. 371–383.
[20] L. Strand, R. Ray, F. Anderson, N. Cohen, Hybrid rocket fuel combustion and regression rate study, in: 28th Joint Propulsion Conference and Exhibit, 1992, p. 3302.
[21] S. Kim, J. Lee, G. Kim, J. Cho, H. Kim, K. Woo, H. Moon, H.-G. Sung, J.-K. Kim, A study on the local regression rate of solid fuel in hybrid rocket, J. Aerosp. Syst. Eng. 2 (2008) 1–6.
[22] G. Cai, Z. Zhao, B. Zhao, Y. Liu, N. Yu, Regression rate and combustion performance investigation on hybrid rocket motor with head-end swirl injection under high geometric swirl number, Aerosp. Sci. Technol. (2020) 105922.
[23] D. Bianchi, F. Nasuti, CFD analysis of hybrid rocket flowfields including fuel pyrolysis and nozzle ablation, in: 49th AIAA/ASME/SAE/ASEE Joint Propulsion Conference, American Institute of Aeronautics and Astronautics, 2013.
[24] C. Li, G. Cai, P. Wang, H. Tian, Flow field and injector heat characteristics of hybrid rocket motor with annular-gap injector, Aerosp. Sci. Technol. 93 (2019) 105326.
[25] M. Bouziane, A. Bertoldi, P. Milova, P. Hendrick, M. Lefebvre, Performance comparison of oxidizer injectors in a 1-kN paraffin-fueled hybrid rocket motor, Aerosp. Sci. Technol. 89 (2019) 392–406.